

Synthesis and photocatalytic activity of nano-sized iron oxides

Ibrahim S. Ahmed¹, Mostafa Y. Nassar², N.Hassan³, Michael B. Azmy³

Abstract— Iron nanoparticles arranged from $\text{Fe}(\text{NO}_3)_3 \cdot 9\text{H}_2\text{O}$ by using chemical precipitation is the methodology used in this work. Materials primarily utilized as a part of this project are iron nitrate nonahydrate (as a basic material), Ammonia solution (as a precipitating material) and product from them calcined at 550°C for 2hrs. The properties i.e. size, morphology and crystallinity of synthesized iron oxide Nanopowders were considered and portrayed by XRD, FTIR, SEM, and TEM. The results of XRD peak confirm the presence of mixed iron oxide nanopowders produced during chemical precipitation and size of as synthesis nanoparticles are 64 nm. TEM come about 61 nm likewise affirms the combination of iron oxide nanoparticles.

Index Terms— Co-precipitation method, nanoparticles, XRD, Fe_2O_3 , photocatalytic degradation, crystal violet dye, XRD.

1 INTRODUCTION

The synthesis of oxide nanoparticles attracts more and more attention because these nanoparticles exhibit electrical, optical and magnetic properties that are different from their bulk counterparts [1]. Iron oxides include $\alpha\text{-Fe}_2\text{O}_3$, $\gamma\text{-Fe}_2\text{O}_3$ and Fe_3O_4 . Among these Iron oxides, $\alpha\text{-Fe}_2\text{O}_3$ has the corundum structure, while the other two have the cubic structure [2, 3]. The study of Iron oxides has attracted intensive attention over the past decades due to the potential applications in catalysts [4-6], gas sensors [7], high density magnetic recording media [8], printing ink [9], ferrofluid [10], magnetic resonance imaging [11] and especially biomedical field [12,13], etc. Photocatalytic processes at semiconductor have received remarkable attention because of their potential application to the conversion of solar energy into chemical energy and pollution control [14]. Various methods have been reported for the synthesis of Iron oxide nanostructures. These methods include reduction of iron salts in micelles [15, 16], thermal reactions [17, 18] using the electrochemical method [19], microemulsion [21], hydrothermal synthesis [22] and sol gel method [23] etc. All these methods to Iron oxide nanostructures are in general complicated and expensive. There are many advantages in the co-precipitation method such as: (a) simple, cheaper and convenient; (b) involve less solvent and reduce contamination; (c) give high yields of products. The photoassisted catalytic degradation of the dyes occurs by the active species created on the surface of metal-oxide semiconductor nanostructures in aqueous solution. In this paper, the iron oxide has been synthesized in basic medium by Simple chemical route and efficiently applied as photocatalyst for the degradation of Cv-dye under light irradiation.

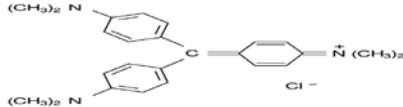
2 EXPERIMENTAL DETAILS

2.1 MATERIALS

The concoction reagents utilized as a part of the present work were ferric nitrate ($\text{Fe}(\text{NO}_3)_3 \cdot 9\text{H}_2\text{O}$), ammonium hydroxide (NH_4OH) and acetic acid (CH_3COOH). All chemicals

were of diagnostic evaluation and with no further filtration. The specification of dye was presented in Table1. Commercially available crystal violet was obtained from oxford, India.

TABLE 1
THE SPECIFICATION OF CRYSTAL VIOLET DYE

Dye	Crystal violet (CV)
Structure	
Molecular formula	$\text{C}_{25}\text{H}_{30}\text{ClN}_3$
λ_{max}	590 nm
Chemical class	Azo compound
C.I. number	42535:3

2.2 PREPARATION OF IRON OXIDE NANOPARTICLES

A salt solution of (1M) of ferric nitrate ($\text{Fe}(\text{NO}_3)_3 \cdot 9\text{H}_2\text{O}$) and (3M) of ammonium hydroxide (the precipitating agent) was gradually blended. The pH of the solution was constantly observed by adding the ammonium solution dropwise. The

reactants were constantly stirred using a magnetic stirrer until a pH level was achieved to 10 using acetic acid. The resultant was stirred for one hour. The prepared brown precipitate were centrifuged for 15 min at 2000 rpm and washed several times with distilled water and then dried over night at above 80 °C. The gained substance was then pounded into a fine powder and then calcined for 2 hrs at 550 °C.

2.3 PHOTOCATALYTIC MEASUREMENTS

The photocatalytic degradation of Crystal violet (Cv) dye was performed under UV light using the illumination of Xenon arc lamp (250 W, $\lambda=380$ nm).

In brief, 0.05 g of as synthesized iron oxide was added in 25 ml of 20 $\mu\text{g}/\text{ml}$ solution of Cv-dye under continuous stirring. The suspension was continuously stirred for 1.30h to obtain the adsorption-desorption equilibrium between Cv-dye and mixed iron oxide (Fe_2O_3 and Fe_3O_4) photocatalyst under dark condition. Finally, UV light illumination was used to stable the aqueous dye suspension under constant stirring. The decomposed dye was taken out after every period and subjected to centrifugation at 4000 rpm to separate out the iron oxides powder. By UV-vis spectrophotometer (JASCO Model V-530) the absorption spectrum of decomposed dye was recorded. The degradation rate of Cv dye over iron oxide is estimated by using equations (1), (2), respectively

$$\text{Photodegradation rate } \% = \text{Ln}\{(A_0 - A_t)/A_0\} \times 100 \quad (1)$$

$$\text{Ln}(A_0/A_t) = k_{\text{app}} t \quad (2)$$

Where, A_0 , A_t is the initial and instant concentration of CV dye at interval time, respectively. From equation (2) the apparent rate constant (k_{app}) for this process could be also estimated.

3 RESULT AND DISCUSSION

3.1 XRD analysis

The phase composition of the as-synthesized materials, iron oxide, was examined utilizing X-ray diffraction analysis. XRD patterns of the iron oxide sample delivered by burning of the dried sample. All the diffraction peaks displayed in Fig. 1 can consummately be ordered to the face centered cubic structure periclase (JCPDS No.89-0598) and (JCPDS No.89-0688). No peaks of other phases were found in the XRD pattern for the product calcined at 550 °C, showing that nanocrystal of the iron oxide prepared by this synthesis method possesses phase of a pure crystalline, which did not appear any impurity, with a space group of $\text{Fm}\bar{3}\text{m}$. Moreover, using the Scherrer equation. The crystallite size (D , nm) of the iron oxide nanoparticles can be calculated [17]:

$$D = 0.9\lambda / \beta \cos\theta_B$$

Where λ is the wavelength of X-ray radiation, β is the full width at half maximum (FWHM) of the diffraction peak and θ_B is the Bragg diffraction angle. The estimated average crystallite size of the as-prepared iron oxide nanoparticles was found to be ca. 64 nm.

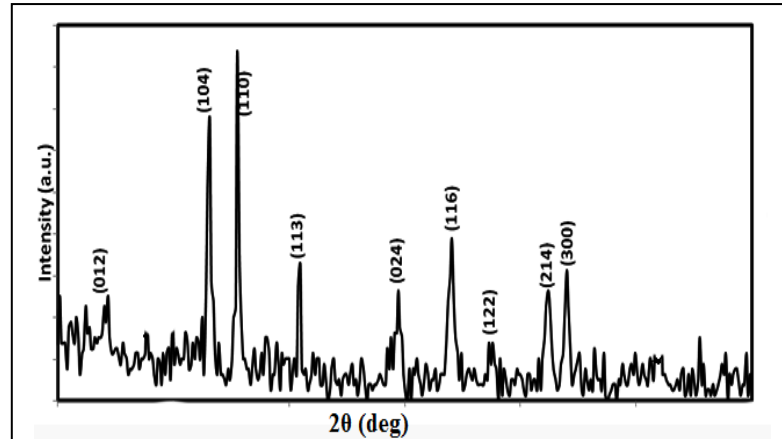


Fig. 1. XRD patterns of iron oxide sample calcined at 550 °C.

3.2 FT-IR

In the IR spectra, the iron oxide sample exhibited characteristic frequency at 437 and 530 cm^{-1} as appeared in fig. 2, respectively, and are connected with the special vibration of Fe_2O_3 which shows the arrangement of iron oxide sample. Nonetheless, In the FTIR spectrum absorption at 3,424 cm^{-1} and 1,635 cm^{-1} is because of O-H stretching and bending vibrations of physically adsorbed H_2O and surface -OH groups [18].

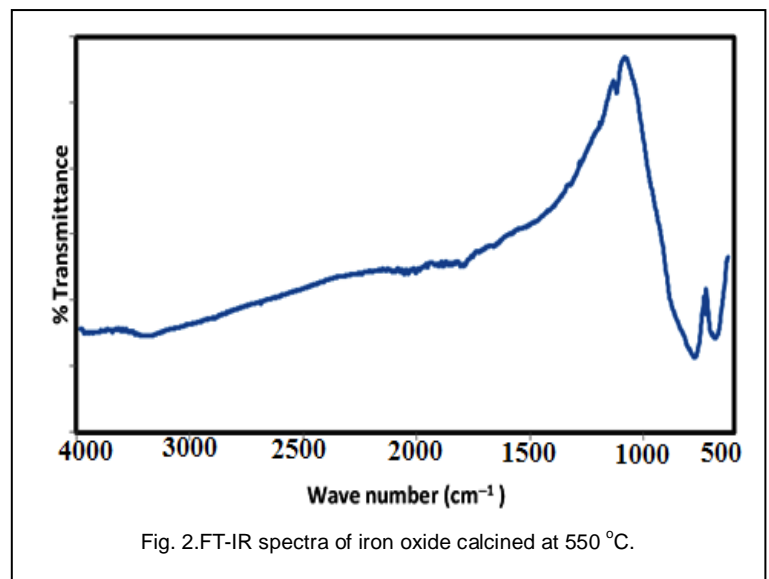


Fig. 2. FT-IR spectra of iron oxide calcined at 550 °C.

3.3 Thermal analysis

The thermal behavior of the precursor samples prepared at pH 10 investigated by TG-DTA, as present in Fig. 3. TGA curve show that the thermal decomposition behavior of the

precursor is decomposed in three steps.

The first step within the temperature range 21 – 126 °C is attributed to elimination of adsorbed/trapped water and the weight loss of this step is found to be 5.8% and this value is close to the calculated value (ca.5.41%).the second step within the temperature range 127 – 385 °C corresponds to the mass loss of 55% and this value is close to the calculated value (ca.55.58%). the third step within the temperature range 386 – 520 °C corresponds to the mass loss of 22% and this value is close to the calculated value (ca.18.4%) to give mixed iron oxides as the final residue.

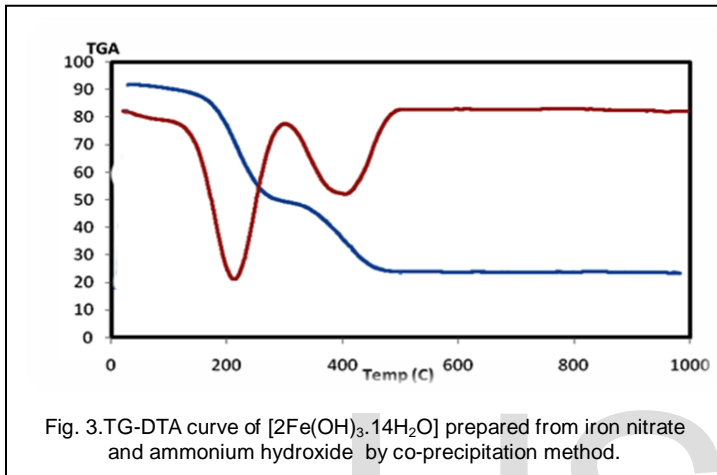


Fig. 3. TG-DTA curve of $[2\text{Fe}(\text{OH})_3 \cdot 14\text{H}_2\text{O}]$ prepared from iron nitrate and ammonium hydroxide by co-precipitation method.

3.4 Energy dispersive x-ray analysis

The EDX of the sample fromed at 550 °C affirmed the nearness of Fe and O as shown in Fig. 4.

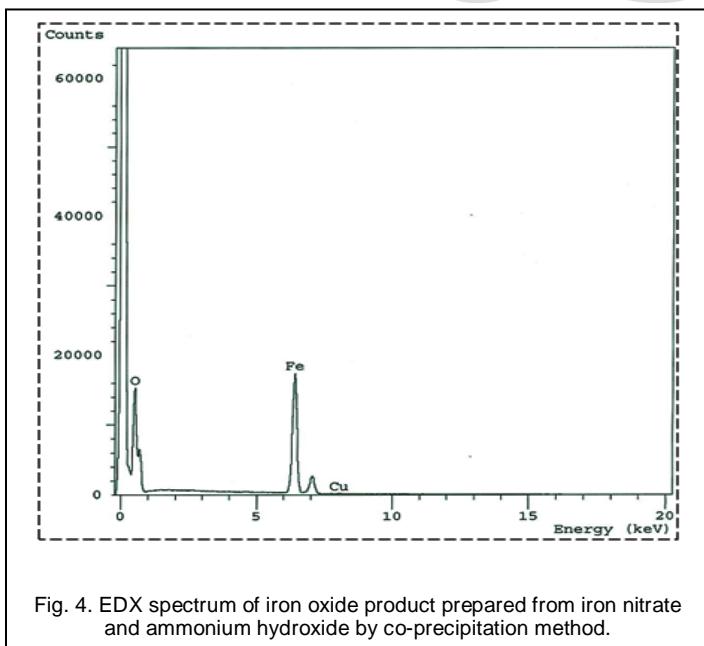


Fig. 4. EDX spectrum of iron oxide product prepared from iron nitrate and ammonium hydroxide by co-precipitation method.

3.5 Field emission scanning electron microscopy (FE-SEM)

Morphologies of the as-prepared iron oxide product calcined at 550 °C were examined by utilizing field emission scanning electron as shown in Fig. 5.

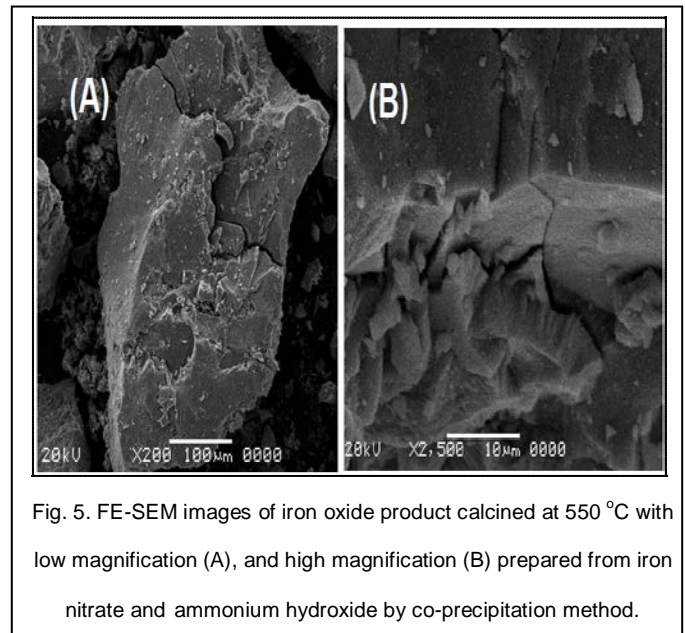


Fig. 5. FE-SEM images of iron oxide product calcined at 550 °C with low magnification (A), and high magnification (B) prepared from iron nitrate and ammonium hydroxide by co-precipitation method.

3.6 HIGH-RESOLUTION TRANSMISSION ELECTRON MICROSCOPY (HR-TEM)

Transmission electron microscope image of iron oxide of the particle was recorded and shown in Fig. 6. The product which is calcined at 550 °C is made out of particles with a normal measurement of 61nm which is near the crystallite size computed from the XRD studies.

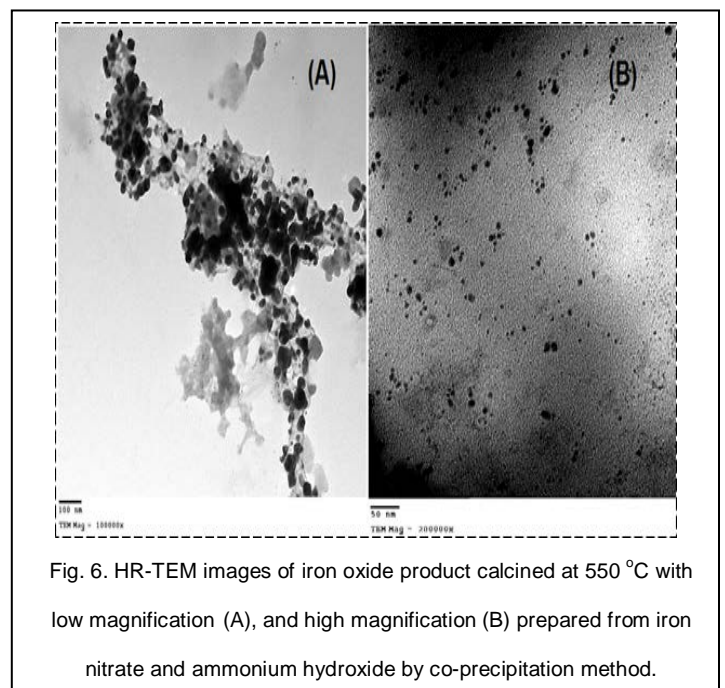


Fig. 6. HR-TEM images of iron oxide product calcined at 550 °C with low magnification (A), and high magnification (B) prepared from iron nitrate and ammonium hydroxide by co-precipitation method.

3.7 OPTICAL ABSORPTION GAP

The optical absorbance properties of the produced iron oxide nanoparticles were investigated by recording UV-Vis absorption spectra. The optical band gap energy (E_g) of iron oxide can be calculated using equation [19]:

$$F(R) = (1-R)^{2/2R}$$

Where R corresponds to a sample of infinite thickness. A more precise value of that parameter is obtained by applying the Pankove formalism [20].

Pankove: $[F(R)]^n$ vs $(h\nu)$; $n = 0.5$ (indirect), $n = 2.0$ (direct)

At Fig. 7 show plotting of $(h\nu)$ versus $F(R)$ of the product, the energy gap found to be 2.588 eV.

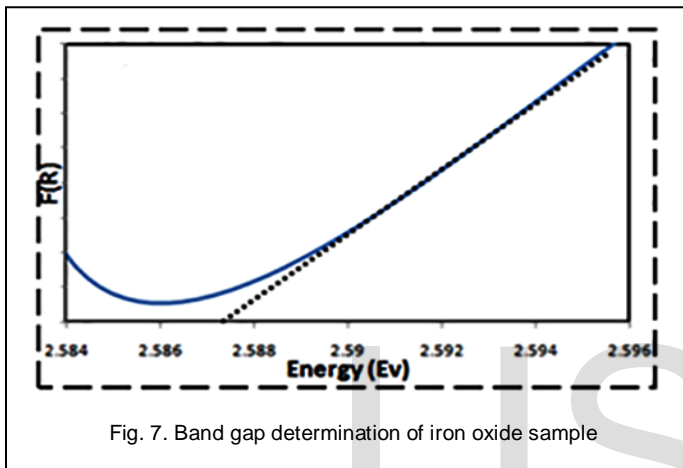


Fig. 7. Band gap determination of iron oxide sample

4. Photocatalytic study

The crystal violet (CV) dye degradation was studied over the surface of mixed iron oxide samples at pH 10 which combustion at 550 °C with 0.5 ml of H_2O_2 under UV illumination to elucidate the photocatalytic activity.

Fig. 8(a) shows UV-VIS spectra of decomposed CV dye with the variation of exposed time from 0 min to 210 min and exhibits the maximum absorption wavelength at 590 nm. A decrease in CV dye concentration is concluded because the absorbance intensities of CV are gradually decreased in the presence of iron oxide nanoparticles with the increase of exposed time. Interestingly, the crystal violet (CV) dye is significantly degraded by ca.86.69% within relatively short exposed time (210 min) as shown in Fig. 8(a).

However, the CV dye color / concentration decreased by only ca.32.33% when the reaction was carried out under dark for 1.30 h. Fig. 8(b) Shows the degree of CV dye degradation in the presence of iron oxide nanoparticles as a function of irradiation time .the relative concentration of CV dye decrease with increased of exposed time. A plot of $\ln(A_0/A_t)$ versus time gives a straight line with a slope as shown in Fig. 8(c)

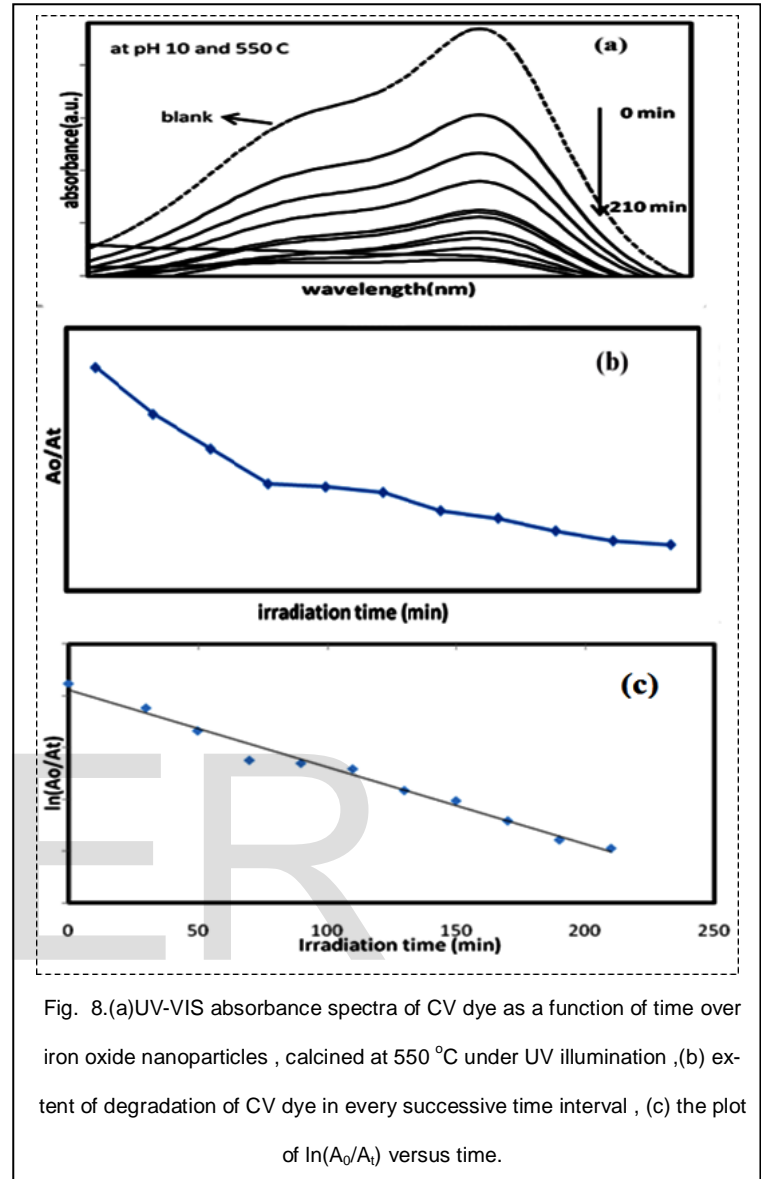


Fig. 8.(a)UV-VIS absorbance spectra of CV dye as a function of time over iron oxide nanoparticles , calcined at 550 °C under UV illumination ,(b) extent of degradation of CV dye in every successive time interval , (c) the plot of $\ln(A_0/A_t)$ versus time.

5. Conclusion

The highly activity iron oxide NPs were synthesized by the solution phase approach with ammonium hydroxide as precipitating agent at 550 °C. The iron oxide NPs were characterized in terms of morphological, structural, and optical properties by FESEM, TEM, EDX, XRD and UV-visible spectrophotometer techniques. The synthesized iron oxide NPs exhibited mono-dispersity with the average size 64 nm.The photocatalytic investigation was carried out by performing the decomposition of CV dye under UV illumination over as-synthesized iron oxide NPs.CV dye was considerably degraded by 86.69% within 210 min over the iron oxide NPs.

6. References

- [1] H. Xu, X. Wang, L. Zhang, Powder Technology, 185 (2008) 176.
- [2] J. Lu, Sh. Yang, K. Ming, Ch. Su, Ch. Yeh, Y. Wu, D. Shieh, Nanotechnology, 17 (2006) 5812.
- [3] X. Batlle, A. Labarta, J. Phys. D: Appl. Phys., 35 (2002) 15.
- [4] D. Huang, D. Cao, Y. Li, H. Jiao, J. Phys. Chem. B, 110 (2006) 13920
- [5] O. Shekhah, W. Ranke, A. Schule, G. Kolios, R. Schlogl, Angew. Chem. Int. Ed. Engl., 42 (2003) 5760.
- [6] M.Y. Nassar, I.S. Ahmed, T.Y. Mohamed, M. Khatab, A controlled, template-free, and hydrothermal synthesis route to sphere-like [small alpha]-Fe₂O₃ nanostructures for textile dye removal, RSC Advances, 6 (2016) 20001-20013.
- [7] M.Y. Nassar, I.S. Ahmed, Template-free hydrothermal derived cobalt oxide nanopowders: Synthesis, characterization, and removal of organic dyes, Materials Research Bulletin, 47 (2012) 2638-2645.
- [8] M.Y. Nassar, I.S. Ahmed, Hydrothermal synthesis of cobalt carbonates using different counter ions: An efficient precursor to nano-sized cobalt oxide (Co₃O₄), Polyhedron, 30 (2011) 2431-2437.
- [9] M.Y. Nassar, Size-controlled synthesis of CoCO₃ and Co₃O₄ nanoparticles by free-surfactant hydrothermal method, Materials Letters, 94 (2013) 112-115.
- [10] H.M. Aly, M.E. Moustafa, M.Y. Nassar, E.A. Abdelrahman, Synthesis and characterization of novel Cu (II) complexes with 3-substituted-4-amino-5-mercapto-1,2,4-triazole Schiff bases: A new route to CuO nanoparticles, Journal of Molecular Structure, 1086 (2015) 223-231.
- [11] L.X. Tifenauer, A. Tschirky, G. Kuhne, R. Andres, Magn. Reson. Imaging, 14 (1996) 391.
- [12] Z. Berkova, J. Kriz, P. Girman, K. Zacharovova, T. Koblas, E.Dovolilova, F. Saudek, Transplant Proc, 37 (2005) 3496.
- [13] F. Mishima, S. Takeda, Y. Izumi, S. Nishijima, IEEE Trans. Appl.Supercond., 16 (2006) 1539.
- [14] J. Zhong,Ch. Cao. Sensors and Actuators B, 145 (2010) 651.
- [15] R.M. Cornell, U. Schwertmann,The Iron Oxides, VCH, NewYork, 1996.
- [16] J.P. Wilcoxon, P.P. Provencio, J. Phys. Chem. B, 103 (1999) 9809.
- [17] C.T. Seip, C. Connor, Nanostruct. Mater., 12 (1999) 183.
- [18] T.W. Smith, D. Wychlck, J. Phys. Chem. B, 103 (1999) 9809.
- [19] J. Van Wonerghem, S. Morup, Phys. Rev. Lett., 55(1985) 410.
- [20] W.Q. Jiang, H.C. Yang, S.Y. Yang, H.E. Horng, J.C. Hung, Y.C. Chen,C.Y. Hong, J. Magn. Magn.Mater., 283 (2004) 210.
- [21] D.E. Zhang, Z.W. Tong, S.Z. Li, X.B. Zhang, A.L. Ying, Mater. Lett.,62 (2008) 4053.
- [22] M.Z. Wu, Y. Xing, Y.S. Jia, H.L. Niu, N.P. Qi, J. Ye, Q.W. Chen,Chem.Phys.Lett., 401 (2005) 374.
- [23] J. Xu, H.B. Yang, W.Y. Fu, K. Du, Y.M. Sui, J.J. Chen, Y. Zeng, M.H.Li, G.G. Zou, J.Magn. Magn.Mater., 309 (2007) 307.
- [24] R. Jenkins and R. L. Snyder, Chemical Analysis: Introduction to X-ray Powder Diffractometry, John Wiley and Sons, Inc. New York (1996).
- [25] Bersani,D.;Lottici,P.P.;Montenero,A. J.RamanSpectrosc. 1999, 30,355.
- [26] P.Kubelka, F.Munk, Tech.Phys.12 (1931)593.
- [27] J.Tauc, R.Grigorovici, A.Vancu, Phys.StatusSolidiB15 (1966)627.

Authors:

1-Ibrahim S. Ahmed

(Faculty of science, Benha University, Benha, Egypt)

Email (isahmed2010@gmail.com)

Mobile (+20 1119294966)

2- Mostafa Y. Nassar

(Faculty of science, Benha University, Benha, Egypt)

Email (m_y_nassar@yahoo.com)

Mobile (+20 1068727555)

3- N.Hassan

(Faculty of science, Portsaid University, Portsaid, Egypt)

Email (nader_yousri1972@yahoo.com)

Mobile (+20 1119952995)

3-Michael B. Azmy

(Faculty of science, Portsaid University, Portsaid, Egypt)

Email (ch.michaeldemetry@gmail.com)

Mobile (+20 1205802120)

IJSER